

PAPER • OPEN ACCESS

## Heat flux measurement approach for an enhanced thermometric method: preliminary tests

To cite this article: L Evangelisti *et al* 2024 *J. Phys.: Conf. Ser.* **2685** 012051

View the [article online](#) for updates and enhancements.



**PRIME**  
PACIFIC RIM MEETING  
ON ELECTROCHEMICAL  
AND SOLID STATE SCIENCE

HONOLULU, HI  
Oct 6–11, 2024

Abstract submission deadline:  
**April 12, 2024**

Learn more and submit!

**Joint Meeting of**

The Electrochemical Society  
•  
The Electrochemical Society of Japan  
•  
Korea Electrochemical Society

# Heat flux measurement approach for an enhanced thermometric method: preliminary tests

L Evangelisti<sup>1,\*</sup>, L Barbaro<sup>1</sup>, E De Cristo<sup>2</sup>, C Guattari<sup>3</sup>, T D’Orazio<sup>3</sup>, F Asdrubali<sup>1</sup> and R De Lieto Vollaro<sup>1</sup>

<sup>1</sup> Roma TRE University, Department of Industrial, Electronic and Mechanical Engineering, Via Vito Volterra 62, 00146 Rome, Italy

<sup>2</sup> Niccolò Cusano University, Department of Engineering, Via Don Carlo Gnocchi 3, 00166 Rome, Italy

<sup>3</sup> Roma TRE University, Department of Philosophy, Communication and Performing Arts, Via Ostiense 139, 00154 Rome, Italy

\* Corresponding author: luca.evangelisti@uniroma3.it

**Abstract.** In situ tests are suitable to confirm the real thermal performance of building components, and several significant on-site measurement techniques have been studied in literature. However, among them the Thermometric (THM) method has been poorly examined by the scientific community, thus having opportunities for improvement, being a quite a new and non-standardized technique. The theory behind this technique is the Newton’s law of cooling and the main issue is associated to the heat transfer coefficient for which there is no agreement about the value to use. Here, a simple experimental apparatus characterized by a vertical heated sample, suitably thermally insulated was realized. Sensors were installed and direct heat flux measurements through a heat flux plate were performed and compared with (i) the heat flows obtained through the THM method (test conducted using the internal heat transfer coefficient recommended by the ISO 6946) and (ii) the heat fluxes obtained through the proposal of an enhanced THM method based on dimensionless groups analysis, thus requiring data processing based on convective and radiative components.

## 1. Introduction

It is known that in situ tests are suitable to confirm the real thermal performance of building components [1]. Theoretical values can vary from the performance evaluated on site, under real thermal boundary conditions [2]. Consequently, experimental tests are necessary for understanding the behavior of building elements, by using measuring tools and methodological approaches appropriate for logging temperatures, heat fluxes and air velocities both for indoor and outdoor environments [3]. Then, a post-processing is required to achieve performance indicators, such as thermal resistance and/or thermal conductance of building components [4].

Different significant on-site measurement techniques have been studied in literature. In particular, the standardized Heat Flow Meter (HFM) method, the Quantitative Infrared Thermography approach (QIRT), the Simple Hot Box HFM method (SHB-HFM) and the so-called Thermometric method (THM)



have been examined by several researchers. The research efforts related to these methods [5] are shown in figure 1 (obtained through Web of Science database).

The THM method covers only 4%, demonstrating that it has been poorly examined in the literature, thus having opportunities for development. The THM method is fairly new, and it is a non-standardized technique [6]. It needs a suitable total internal heat transfer coefficient for the heat flux calculation, according to the Newton's law of cooling. However, there is no agreement regarding the value to use for the heat transfer coefficient [7].

As a direct solution, considering horizontal heat flows, the heat transfer coefficient proposed by the standard ISO 6946 could be used. It is a constant value, equal to  $7.69 \text{ W/m}^2\text{K}$ , composed by a convective part of  $2.5 \text{ W/m}^2\text{K}$  and a radiative component of  $5.19 \text{ W/m}^2\text{K}$  [8]. Nonetheless, the issue is whether these values are representative for any indoor environmental conditions.

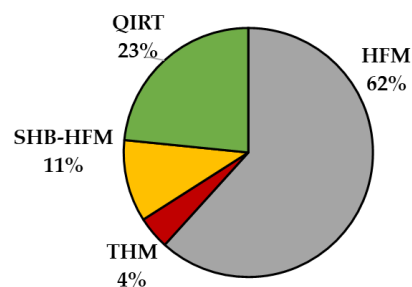


**Figure 1.** Literature analysis related to the in-situ measurement techniques.

The heat exchange between fluids and solids can be evaluated as a function of the surface thermal resistance, and its assessment requires the knowledge of different factors. Obtaining the correct value is challenging, involving appropriate experimental setup [9]. The identification of appropriate heat transfer coefficients is related to the issues of assessing thermal comfort and energy consumption of buildings.

Starting from this, here preliminary experimental tests were conducted as the first step of a wider research activity that aims to make a comparison between the standardized HFM method and the THM method. A simple low-cost experimental apparatus characterized by a vertical sample heated through a heating mat in the rear part, suitably thermally insulated to generate a one-dimensional heat flux was realized. Sensors were installed on the front free surface. Direct heat flux measurements through a heat flux plate were performed and compared with (i) the heat flows obtained through the THM method (test conducted using the internal heat transfer coefficient recommended by the ISO 6946) and (ii) the heat fluxes obtained through the proposal of an enhanced THM method based on dimensionless groups analysis, thus requiring a data processing based on convective and radiative components.

The aim of this work is to lay the groundwork for overcoming the disagreement related to the value of the total heat transfer coefficient in the THM method by proposing an alternative approach.

## 2. Materials and methods

### 2.1 The experimental setup

A simple low-cost experimental apparatus characterized by a vertical sample heated through a heating mat in the rear part, suitably thermally insulated was realized. In particular, 5 cm thickness XPS panels (characterized by a thermal conductivity of about  $0.035 \text{ W/mK}$ ) were shaped and assembled to create an insulating structure where the sample (made of poplar wood, with an unknown thermal conductivity) can be put into. The whole assembly was enclosed using wood panels to guarantee a higher structural stability. The internal XPS insulating structure has a square shape ( $60 \times 60 \text{ cm}$ ) and a thickness of 10 cm (overlapping of two 5 cm XPS layers). The central part has a thickness of 5 cm for housing the sample (whose dimensions are  $30 \times 30 \text{ cm}$ ). One side of the structure can be removed to enable the

sample, the heating mat, and sensors installations, respectively. Figure 2 shows the inner XPS assembly, the external cladding, and the exploded view of the whole structure. The heating mat is characterized by a flexible polyester heating film manufactured by ALPER (dimensions equal to 28 x 28 cm, 16W, 230V, with a thickness of 0.1 cm).

The following sensors were applied and used within a methodological approach for evaluating direct and indirect heat flux measurement techniques: (i) surface temperature sensors were applied to measure the rear surface temperature of the wooden sample; (ii) a thermal imaging camera was used to evaluate the front surface temperature of the sample; (iii) a heat flux sensor was installed for direct heat flow measurements; (iv) a surface temperature probe and (v) a hot-wire anemometer were used to compute the heat flux through an indirect approach. Table 1 lists the main technical characteristics of the equipment. Figure 3 shows a schema of the overall experimental apparatus.



**Figure 2.** Internal XPS structure (a); external cladding (b); exploded view of the structure (c).

**Table 1.** Technical features of the equipment.

Sensor/measurement instrument	Manufacturer	Model	Measuring range	Resolution
Heat-flux sensor	Hukseflux	HFP01	-2000 to 2000 W/m <sup>2</sup>	60 x 10 <sup>-6</sup> V/(W/m <sup>2</sup> )
Surface temperature sensor	LSI	EST124	-60 to +80 °C	0.01 °C
Air temperature sensor	LSI	EST033	-50 to 70 °C	0.01 °C
Hot-wire anemometer	TESTO	0628 0152	0 to 5 m/s	0.01 m/s
Thermal imaging camera	Fluke	Ti480 PRO	-10 to 1000 °C	0.1 °C

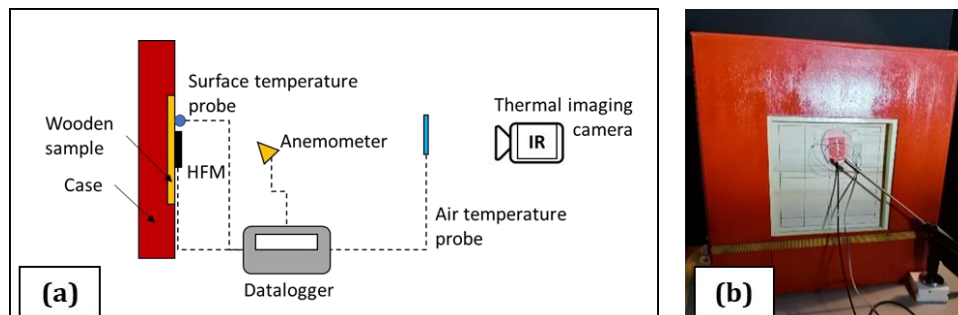


**Figure 3.** Schematic view of sensors installation (a); the actual experimental apparatus (b).

## 2.2 Methodology

The methodological approach is characterized by the following steps:

1) the heating mat was turned on until steady state conditions were reached, and 9 surface temperature sensors were preliminary applied on the rear surface of the wooden sample for measuring the surface temperature (3 equidistant sensors on 3 equidistant lines, within a 3x3 matrix characterized by a spacing

of 7 cm). Moreover, a thermal imaging camera was used to assess the front surface temperature of the sample for obtaining data about the temperature distribution of the front free surface. In order to obtain reliable results, the emissivity of the wooden sample was obtained by comparing surface temperature values measured through a surface temperature probe and the thermal imaging camera itself. This approach allowed us to identify an emissivity of the wooden sample equal to 0.84.

2) Due to the hypothetically inhomogeneous heating of the sample, a calibrated Comsol 3D model was created to evaluate possible heat flux deviations from one-dimensional conditions, thus identifying the best position for installing the heat flux sensor and the surface temperature probe. The calibration procedure was done by calculating the model efficiency ( $EF$ ) index [10]:

$$EF = \frac{\sum_{i=1}^N (m_i - \bar{m})^2 - \sum_{i=1}^N (s_i - m_i)^2}{\sum_{i=1}^N (m_i - \bar{m})^2} \quad (1)$$

where  $m_i$  is the measured value at time  $t_i$ ,  $s_i$  is the simulated value for each time  $t_i$  and  $N$  is the total number of samples. In addition,  $\bar{m}$  is the mean value among the measured ones.  $EF$  ranges between 0 and 1. When it is equal to 1, the measured and simulated values are identical. Once the model was calibrated based on the temperatures measured by the thermal imaging camera (with an expected  $EF$  value greater than 0.9), Comsol was used to simulate the distribution of the heat flux on the sample. In this way, the best position for installing the sensors was identified.

3) Once the stationary conditions have been reached, the heat flux sensor was used for direct heat flow density measurements ( $q_{HFM}$ ).

4) At the same time, data logged by the surface and air temperature probes and data acquired through the hot-wire anemometer was used to calculate the convective coefficient through the dimensionless groups analysis [9]. Three distances (5, 6 and 7 cm from the sample) were preliminary tested in order to comprehend the influence of the anemometer position. Distances of less than 5 cm have not been tested due to the protective structure of the anemometer. Grashof ( $Gr$ ) and Reynolds ( $Re$ ) numbers were estimated, and the Archimedes ( $Ar$ ) number allowed to understand the specific convection conditions:

$$Ar = \frac{Gr}{Re^2} \quad (2)$$

It is known that if  $Ar$  is lower than 0.7 the convection is forced; if  $Ar$  is much greater than 10 the convection is natural. Lastly, if  $Ar$  is in the range of 0.7 to 10, the convection is mixed. In natural convection, the convective heat transfer coefficient ( $h_c$ ) can be obtained through the Nusselt number ( $Nu$ ), which is a function of the Rayleigh ( $Ra$ ) number. Considering vertical surfaces, the equations below [11] can be applied:

$$Nu = 0.59 \cdot Ra^{\frac{1}{4}}, \quad 10^4 < Ra < 10^9 \quad (3)$$

$$Nu = 0.10 \cdot Ra^{\frac{1}{3}}, \quad 10^9 < Ra < 10^{13} \quad (4)$$

$Nu$  is defined as a function of  $h_c$  and the geometrical characteristic length (equal to the vertical length of the wooden sample, of 0.30 m).

5) The radiative heat transfer coefficient ( $h_r$ ) was computed according to the following equation:

$$h_r = 4\varepsilon\sigma T_m^3 \quad (5)$$

where  $\varepsilon$  is the emissivity of the sample,  $\sigma$  is the Stefan-Boltzmann constant and  $T_m$  is the average thermodynamic temperature of the surface and the surrounding surfaces (considered as the average between the wooden sample surface temperature and the air temperature measured far from the specimen) [8].

6) The heat flux density was calculated by applying the Newton's law of cooling ( $q_{THM}$ ):

$$q_{THM} = h_{tot} \cdot (T_s - T_{air}) \quad (6)$$

where  $T_s$  and  $T_{air}$  are the surface temperature of the wooden sample and the air temperature, respectively, and  $h_{tot}$  is the total heat transfer coefficient, obtained as the sum of the convective and radiative component. The heat flux obtained from equation (6) was named  $q_{THM}$  because this formula must be applied when the THM method is used for wall thermal characterization.

7) Finally,  $q_{HFM}$  and  $q_{THM}$  were compared, also considering the widely used  $h_{tot}$  value equal to  $7.69 \text{ W/m}^2\text{K}$ , recommended by the standard ISO 6946.

A preliminary uncertainty analysis in terms of repeatability was carried out, considering a coverage factor of 2, which implies approximately 95% confidence.

### 3. Results and discussion

According to the methodological approach, stable operating conditions were reached during the experimental campaign. During the first step, 9 surface temperatures and thermographic images were acquired. In this phase, an inhomogeneous heating of the sample was observed, with higher temperatures in its upper part. Given the limitation of the heating mat's capacity to uniformly heat the sample, the thermal image was processed (adapting the temperature scale) to identify the best position for the installation of the heat flow sensor. In particular, this position was identified highlighting the sample area that had a temperature difference of less than  $2^\circ\text{C}$  (see figure 4a). Then, considering the thermal image with the original temperature scale (relative to the whole sample), two perpendicular virtual lines crossing the previously identified region (called L0 and L1, as shown in figure 4b) were created using the thermographic image processing software, thus obtaining the associated temperatures. Starting from the obtained temperature data, the wooden sample was modelled through Comsol aiming at simulating the heat fluxes crossing the sample. The 3D model was calibrated using as input the rear temperatures and exploiting the front temperatures measured by the thermal imaging camera on L0 and L1. The obtained values for the EF index were respectively 0.945 referring to the vertical line (L0) and 0.988 referring to the horizontal one (L1), thus highlighting a good agreement between experimental measurements and simulation.

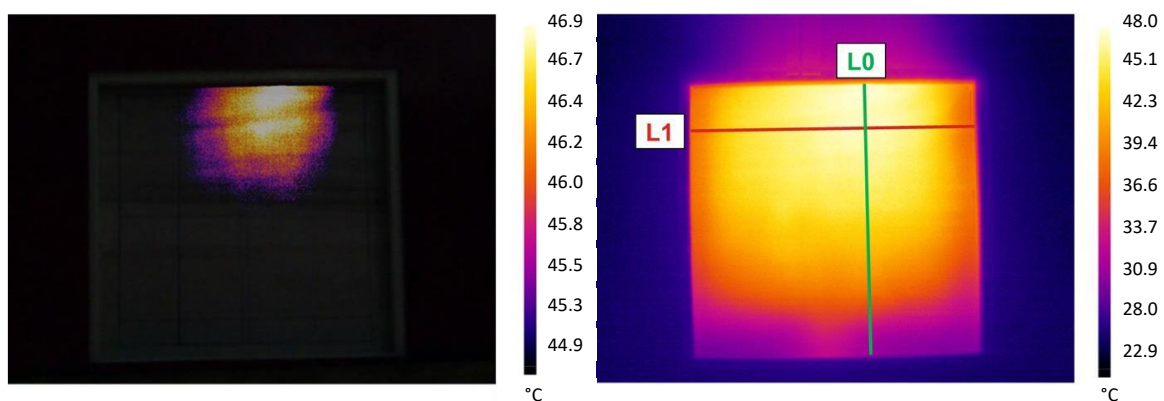


**Figure 4.** Area where the  $\Delta T$  is at most  $2^\circ\text{C}$  (a); virtual lines for the calibration procedure (b).

Consequently, the heat fluxes along L0 and L1 were simulated using Comsol, and the  $x$ ,  $y$  and  $z$  heat flux components (see figure 5a) were evaluated to identify the best position for installing the sensors. In particular, the condition applied to evaluate the heat flux distortion was that the  $x$  and  $z$  components of the heat flux had to be less than 5% of the  $y$  component. This condition was satisfied within the green area shown in figure 5b.

Data derived from the heat flux sensor ( $q_{HFM}$ ), the surface ( $T_s$ ) and air temperature ( $T_{air}$ ) probes and data acquired through the hot-wire anemometer ( $u$ ), were processed to define the convection mode. The



obtained values are reported in Table 2. For an average film temperature of 30.94 °C, it was considered a thermal conductivity equal to 0.02641 W/mK, a kinematic viscosity equal to  $1.61 \cdot 10^{-5} \text{ m}^2/\text{s}$ , a thermal expansion coefficient of  $3.29 \cdot 10^{-3} \text{ 1/K}$  and a Prandtl number ( $Pr$ ) equal to 0.714. The dimensionless parameters approach allowed to obtain the results listed in Table 3, where only average values are listed.

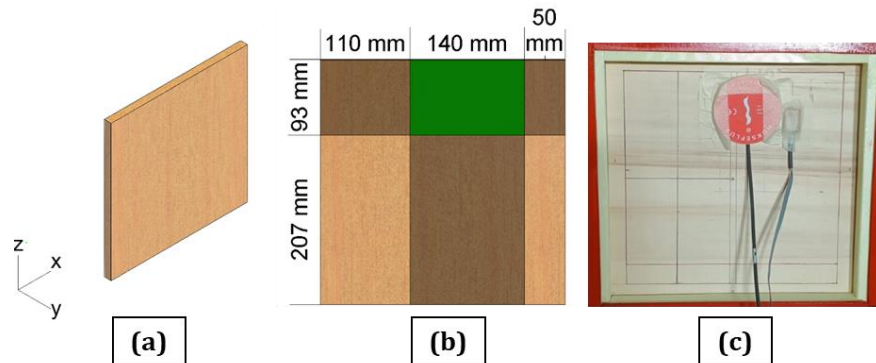


**Figure 5.** Sample and coordinate system (a); green area, characterized by one-dimensional heat flux according to the Comsol model (b); heat flux and surface temperature sensors (c).

**Table 2.** Operating conditions of experimental campaign.

Anemometer distance [cm]	$q_{HFM}$ [W/m <sup>2</sup> ]	$T_s$ [°C]	$u$ [m/s]	$T_{air}$ [°C]
5	180.34±0.37	40.27±0.01	0.08±0.01	21.57±0.02
6	182.33±0.34	40.39±0.01	0.08±0.01	21.50±0.01
7	183.78±0.23	40.43±0.01	0.08±0.01	21.45±0.01

**Table 3.** Dimensionless parameters average values.

Anemometer distance [cm]	$Gr$	$Re$	$Ar$	$Ra$	$Nu$
5	$6.27 \cdot 10^7$	$1.40 \cdot 10^3$	34.24	$4.47 \cdot 10^7$	48.25
6	$6.33 \cdot 10^7$	$1.42 \cdot 10^3$	34.05	$4.52 \cdot 10^7$	48.37
7	$6.36 \cdot 10^7$	$1.43 \cdot 10^3$	33.90	$4.54 \cdot 10^7$	48.42

The convection is purely natural for each tested distance of the anemometer because the  $Ar$  is constantly much greater than 10. Starting from this, the convective heat transfer coefficients ( $h_c$ ) were found through the Nusselt number ( $Nu$ ), considering vertical surfaces. From the calculation of the  $Ra$  number, equation (3) was applied. The radiative heat transfer coefficient ( $h_r$ ) was computed according to equation (5) and the heat flux density ( $q_{THM}$ ) was calculated by applying the Newton's law of cooling by means of equation (6). The results listed in Table 4 allow to observe that the distance of the anemometer has a negligible influence. As stated before, distances less than 5 cm have not been assessed due to the protective structure of the anemometer (see figure 3b).

It is worthy to observe that the obtained average total heat transfer coefficient of about 9.61 W/m<sup>2</sup>K is quite different from that suggested by the standard. It is related to the specific temperature differences between sample and air which in this case differ widely from the values that can occur when a real wall is analyzed. However, this comparison highlights the need for an experimental approach to identify suitable convective and radiative heat transfer coefficients, useful for obtaining appropriate values to be used in the thermal characterization of envelope components when the THM method is to be applied.

All this brings us back to the main problem of the THM method, associated with the heat transfer coefficient for which there is no agreement on the value to use. In this case, using the value recommended by the standard would imply percentage differences equal to about -20%. For this reason,  $q_{THM}$  values were compared both with the data logged by the heat flux sensor ( $q_{HFM}$ ) and the heat flux computed applying the  $h_{tot}$  value equal to 7.69 W/m<sup>2</sup>K, recommended by the ISO 6946 (named  $q_{ISO}$ ). The results are shown in Table 5.

The obtained results allowed to calculate extremely low percentage differences between the THM and HFM method. For a distance of 5 cm of the anemometer, the percentage differences ranged between about -2% and +2%. For the distances of 6 cm and 7 cm similar values were found, with percentage variations ranging between about -4% and +1%.

Higher percentage differences were found by comparing the use of the  $h_{tot}$  suggested by the standard and the HFM method. In this case, variations ranging from about -23% to -18% were obtained.

**Table 4.** Convective and radiative heat transfer coefficients, and heat flux for the THM approach.

Anemometer distance [cm]	$h_c$ [W/m <sup>2</sup> K]	$h_r$ [W/m <sup>2</sup> K]	$h_{tot}$ [W/m <sup>2</sup> K]	$q_{THM}$ [W/m <sup>2</sup> ]
5	4.25±0.01	5.356±0.002	9.60±0.01	179.64±0.56
6	4.26±0.01	5.357±0.001	9.62±0.01	181.67±0.25
7	4.26±0.01	5.357±0.001	9.62±0.01	182.59±0.19

**Table 5.** Heat fluxes obtained through the direct and indirect approach.

Anemometer distance [cm]	$q_{HFM}$ [W/m <sup>2</sup> ]	$q_{THM}$ [W/m <sup>2</sup> ]	$q_{ISO}$ [W/m <sup>2</sup> ]
5	180.34±0.37	179.64±0.56	143.85±0.34
6	182.33±0.34	181.67±0.25	145.30±0.16
7	183.78±0.23	182.59±0.19	145.95±0.12

#### 4. Conclusions

The aim of this work was to lay the grounds for overcoming the disagreement regarding the value of the total heat transfer coefficient when the THM method is applied. Here, an alternative method based on the dimensionless groups' evaluation was proposed. A simple experimental setup was built, and direct and indirect heat flux measurements were conducted. The measurements were made by applying a heat flux sensor and the results were compared with the heat fluxes obtained through the THM method. The tests were performed both using the conventional total heat transfer coefficient suggested by the ISO 6946 standard, and through the proposal of an advanced THM method based on the evaluation of the convective and radiative heat transfer coefficients.

The results showed that the THM method can provide satisfying results in terms of indirect heat flux measurements, showing extremely low percentage differences if compared with the HFM method (variations ranging from -4% to +2%). Consequently, these preliminary results allowed to affirm that the THM method has chances for improvement, needing further investigations and aiming at providing new measurement systems able to evaluate heat fluxes through an indirect approach. A measurement system able of autonomously calculating the heat transfer coefficient according to the specific thermo-fluid dynamic conditions would allow users to be freed from potentially inappropriate choices. The results highlighted that using the total heat transfer coefficient value suggested by the ISO 6946 lead to lower heat flux values, with percentage variations of about -20% on average.

Future developments will be related to the optimization of the experimental apparatus thus obtaining a more homogeneous distribution of temperatures on the sample, and the application of this



methodological approach to real case studies. On the other hand, due to the thermal and fluid dynamic phenomena, the position of the hot wire anemometer will be examined more in depth.

## 5. References

- [1] Flores Larsen S, Hongn M, Castro N and González S 2019 Comparison of four in-situ methods for the determination of walls thermal resistance in free-running buildings with alternating heat flux in different seasons *Constr. Build. Mater.* **224**, pp 455-473
- [2] Desogus G, Mura S and Ricciu R 2011 Comparing different approaches to in situ measurement of building components thermal resistance . *Energy Build.* **43** pp 2613–20
- [3] Nardi I and Lucchi E 2023 In Situ Thermal Transmittance Assessment of the Building Envelope: Practical Advice and Outlooks for Standard and Innovative Procedures. *Energies* **16** 3319
- [4] Evangelisti L, Guattari C, De Lieto Vollaro R and Asdrubali F 2020 A methodological approach for heat-flow meter data post-processing under different climatic conditions and wall orientations. *Energy Build.* **223** 110216
- [5] Bienvenido-Huertas D, Moyano J, Marí D and Fresco-Contreras R 2018 Review of in situ methods for assessing the thermal transmittance of walls. *Renew. Sustain. Energy Rev.* **102** pp 356–371
- [6] Teni M, Krstić H and Kosiński P 2019 Review and comparison of current experimental approaches for in-situ measurements of building walls thermal transmittance. *Energy Build.* **203** 109417
- [7] Evangelisti L, Scorza A, De Lieto Vollaro R and Sciuto S A 2022 Comparison between Heat Flow Meter (HFM) and Thermometric (THM) Method for Building Wall Thermal Characterization: Latest Advances and Critical Review *Sustainability* **14** 693
- [8] *ISO 6946:2017* 2017 Building Components and Building Elements—Thermal Resistance and Thermal Transmittance—Calculation Methods. International Organization for Standardization (ISO): Geneva Switzerland
- [9] Evangelisti L, Guattari C and De Rubeis T 2021 Preliminary analysis of the influence of environmental boundary conditions on convective heat transfer coefficients, *J. Phys. Conf. Ser.* **1868** 012024.
- [10] Loague K and Green R E 1991 Statistical and graphical methods for evaluating solute transport models: overview and application, *J. Contam. Hydrol.* **7** pp 51–73.
- [11] Bergman T L, Lavine A S, Incropera F P and Dewitt D P 2017 *Fundamentals of Heat and Mass Transfer* John Wiley & Sons.